Measurements of secondary particles emitted by ^{12}C, ^{4}He and ^{16}O ion beams in view of innovative dose profiling technique in Particle Therapy

A. Rucinski[b,d], G. Battistoni[g], F. Collamati[a,b], E. De Lucia[c], R. Faccini[a,b], M. Marafini[a,b], I. Mattei[g], S. Muraro[g], R. Paramatti[b], V. Patera[b,d,e], D. Pinci[b], A. Russomando[a,b,f], A. Sarti[c,d,e], A. Sciubba[b,d,e], E. Solfaroli Camillocci[a], M. Toppi[c], G. Traini[a,b], C. Voena[a,b]

[a] Dipartimento di Fisica, La Sapienza Università di Roma, Roma, Italy [b] INFN Sezione di Roma, Roma, Italy [c] Laboratori Nazionali di Frascati dell'INFN, Frascati, Italy [d] Dipartimento di Scienze di Base e Applicate per Ingegneria, La Sapienza Università di Roma, Roma, Italy [e] Museo Storico della Fisica e Centro Studi e Ricerche "E. Fermi", Roma, Italy [f] Center for Life Nano Science@Sapienza, Istituto Italiano di Tecnologia, Roma, Italy [g] INFN Sezione di Milano, Milano, Italy

Abstract

Hadrontherapy is a technique that uses accelerated charged ions for cancer treatment. The high irradiation precision and conformity achievable during hadrontherapy treatments allows for local tumor control and sparing of the surrounding healthy tissues. Such a high spatial selectiveness requires the development of new dose monitoring techniques.

It has been proved that the beam emits secondary particles in the path to the tumor, namely γ from β^{+} emitters, prompt γ from nuclear de-excitation and charged particles, that can be used to monitor Bragg Peak (BP) position and the related dose release.

In this contribution preliminary results obtained in the study on the neutral and charged secondary particles produced by ^{12}C , ^{4}He and ^{16}O ion beams of therapeutical energy impinging on PMMA phantoms will be presented. The data acquisition have been performed at GSI (Darmstadt, Germany) and HIT (Heidelberg, Germany) facilities. A correlation between the secondary generation regions and BP position will be shown and the design of a monitoring device exploiting all the secondary information will be outlined.

1. Introduction

Currently about 50 radiotherapy centers using proton and/or carbon ion beams for treatment of solid tumors are in operation around the word and several others are under construction or in the planning phase [1]. The benefit from application of ion pencil beams for radiotherapy is related to (i) their favorable, inversed in comparison with photons dose deposition profile (Bragg Peak - BP), (ii) reduced scattering due to the application of active scanning technique for beam delivery and (iii) increased in comparison to photons Radiobiological Effectiveness (RBE) resulting from high Linear Energy Transfer (LET) of those beams [2]. Recent research discussions consider the use of Helium and Oxygen beams for radiotherapy and few synchrotron based hospital centers offer those ions for research, mainly for the radio-biological studies [3]. Helium beams are considered as a compromise between the high LET of Carbon ions and low LET in plateau region of Protons, which could be an optimal solution for the treatment of radio-resistant tumors of pediatric patients [4]. The increased LET characteristic of Oxygen beams, exceeding the LET of Proton, Helium and Carbon beams, is expected to improve efficiency of radio-resistant tumor treatments.

Independently of the ion beam used for treatment, major drawbacks of scanned pencil beam delivery (typical longitudinal profile up to teens of millimeters) in comparison with a passive, broad beam approach, are related to the high sensitivity of this technique to the patient mis-positioning and anatomy variations. For this reason, one of the crucial research aspects of hadrontherapy is a development of on-line monitoring techniques allowing real time control of the beam range and dose released per raster point. The presence of such techniques in clinical routine would potentially allow for a reduction of the treatment planning margins and/or application of unconventional irradiation fields, which normally cannot be used due to the proximity of critical organs at risk located after the distal fall-off of the BP [5]. So far, the most established monitoring technique for ion therapy is based on the detection of the back-to-back photons produced by the annihilation of positrons coming from β^+ emitters generated by the beam interaction with the patient, typically using Positron Emission Tomography (PET). However, the obtained information is indirect, and the signal level is lower in comparison with PET signals known from clinical diagnostics, which indicates a need for investigation on other methods [6]. Recent developments focus on the detection of particles produced by the beam interaction in the target, in particular charged particles, originating from the projectile and target fragmentation and prompt photons from nucleus de-excitation [7, 8].

The measurements presented here were performed with PMMA target and confirm substantial photon and charged secondary production from ^{12}C, ^{4}He and ^{16}O beams at 90°and 60°with respect to the primary beam direction. This information is required to calibrate and operate the multimodal dose profile monitor which is currently assembled in our group and will be installed in the Centro Nazionale per l'Adroterapia Oncologica (CNAO) in Pavia, Italy. The monitor system will be composed of a two PET heads module, for online monitoring of the β^+ emitters production, and of a range monitor detector able to detect, track and measure energy of both secondary charged particles and prompt gammas (Fig. 1 right).

2. Experimental setup

The test beam was performed in the experimental cave of Heidelberg Ion Beam Therapy Center (HIT) and the obtained results were compared with the previously published results of the experiments performed with Carbon beams at 80 MeV/u in Catania, IT [9, 10] and 220 MeV/u in Darmstadt, DE [7, 8]. At HIT several millions of collisions of Helium (102, 125 and 145 MeV/u), Carbon (120, 160, 180, 220 MeV/u) and Oxygen (210, 260, 300 MeV/u) beams with PMMA targets were registered and secondary production was measured at large angles with respect to the primary beam direction (90°and 60°). Those angular configurations are considered as optimal for dose monitoring as the spatial resolution in the fragment emission point improves with the emission angle, even if the emission statistics worsens and multiple scattering of particles inside the target increases at the large angles with respect to the primary beam direction [7].

The target box with a 4.8x4.8 cm^2 face orthogonal to the beam line was positioned at the beam isocenter $\sim$1 m away from the beam nozzle. The primary beam rate impinging the PMMA target was measured with a 0.2 cm thin plastic scintillator (Start Counter, SC) read out by two opposite Hamamatsu H10580 photomultiplier tubes. The angular distribution of the secondary particles produced in the target were studied by three isocentrically positioned detectors mounted on a movable support: (i) 0.1 cm-thick plastic scintillatior (LTS), (ii) 21 cm-long drift chamber (DC) and (iii) an array of four LYSO 1.5x1.5x12 cm^3 crystals [9, 10, 12]. The primary energy of the beam and PMMA target length (7.65, 10.0, 12.65 cm) were selected in such a way, that the BP position was in-line with the center of LTS, DC and LYSO detectors. For ^{12}C beam PMMA target at one length (10 cm) was used. The DC [11], consisting of six alternated horizontal and six vertical wire layers, was used for three dimensional reconstruction of the charged secondaries tracks [7]. The readout and performances of the DC as well as the tracking algorithm and DC calibration have been reported elsewhere [10]. The sketch of the experimental setup is shown in Fig. 1 (left).

Time and charge information from all described above detectors have been used to select prompt

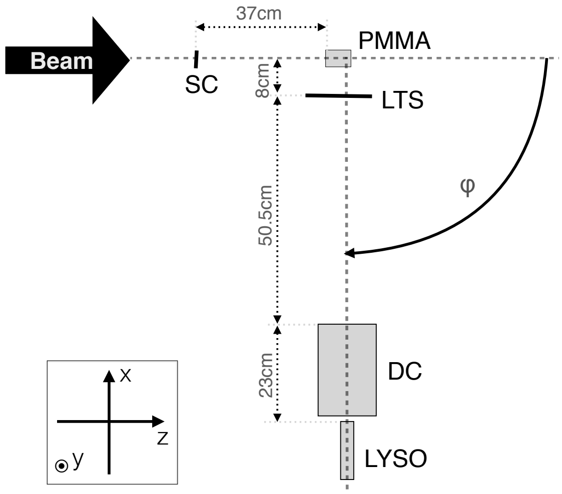

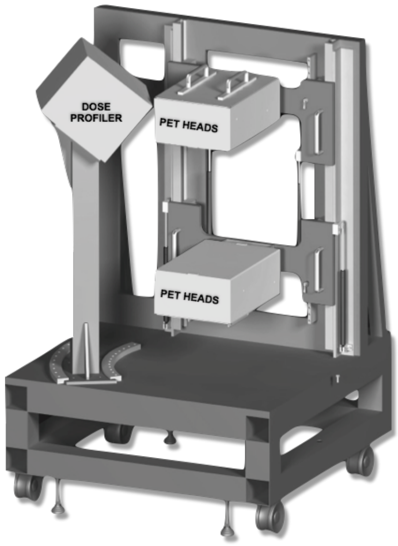

Fig. 1: LEFT: Experimental setup at HIT. Beam - primary beam, SC - start counter, PMMA - target, LTS - plastic scintillator, DC - drift chamber, LYSO - matrix of four LYSO crystals, φ - angular configuration of movable support with LTS, DC and LYSO detectors (90°and 60°with respect to the primary beam). The coordinate system is plotted in the box on the bottom left side of the figure. BP was expected within the PMMA target at the intersection of the dashed lines for ^{12}C at 220 MeV/u, ^{4}He and ^{16}O beams. **RIGHT**: A sketch of the multi-modal in-beam dose monitor able to detect at the same time, back-to-back gammas from β+ annihilation (PET HEADS, not covered in this contribution), charged secondary particles emerging from the patient and prompt gammas with energies higher than 1 MeV (DOSE PROFILER).

gamma and charged secondaries. The lateral profile of the primary beams (FWHM) was $\sim$1 cm. The trigger was performed by requiring SC and LYSO coincidence within 100 ns. The maximal beam rate was of few MHz whereas the maximal trigger rate was $\sim$10 kHz.

3. Preliminary results

3.1 Charged secondaries

The charged secondary particles were selected by exploiting the DC information together with the energy released in the LYSO detector. In addition the kinetic energy of the particle was estimated from Time of Flight (TOF) calculated as the time difference between LTS and LYSO signals. Figure 2 (left) shows the number of DC cells (N_{hit}) fired by charged secondary particles produced in the 90° setup configuration by the 220 MeV/u Carbon beam. Most of the events cross all the DC planes, which appears as a peak for N_{hit}=12. The charged particles tracks were reconstructed requiring at least eight cells fired in the DC.

The particle identification was performed by selecting the events on the plot of charge released in LYSO as a function of TOF of the particle. A non negligible production of charged fragments at large angles is observed for all beam types. The emission shape reconstructed from the tracked particles can be correlated to the beam entrance window and the Bragg Peak position as it was already discussed elsewhere [7]. In Fig. 2 (right) the reconstructed emission positions of the charged fragments projected along the beam direction (longitudinal profile; y-z plane) for the Carbon beams of all the exploited energies is shown for 90° setup configuration.

The reconstructed emission position projected perpendicularly to the beam direction (lateral pro-

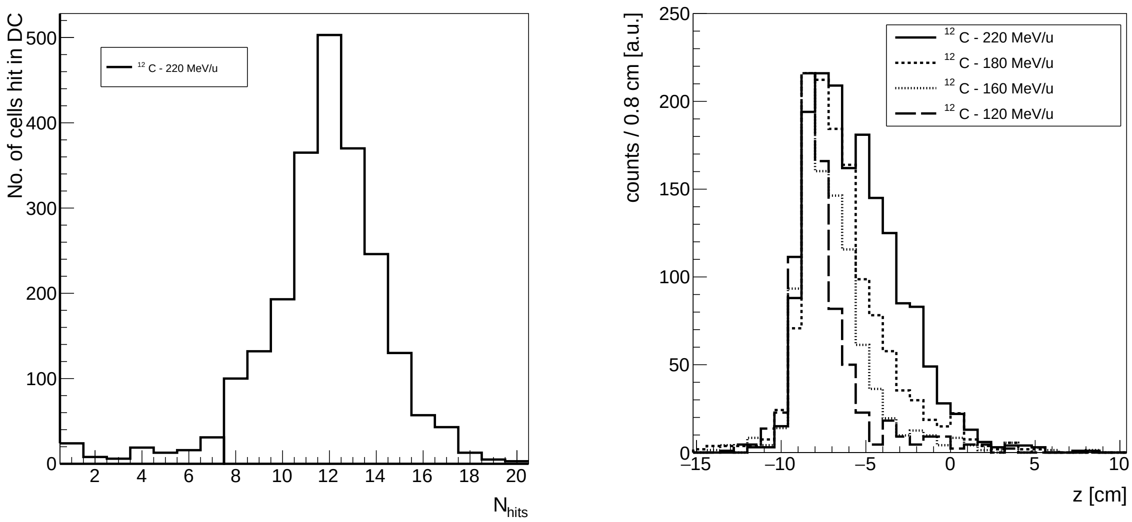

Fig. 2: LEFT: Distribution of the number of cells hit in the DC (N_{hit}) for secondary charged particles emitted from the interactions of ^{12}C beams with the PMMA target. The peak at N_{hit}=12 is an indication of a charged particle that went trough all the DC planes. **RIGHT**: Emission profiles of secondaries produced by Carbon beam at different energies. The PMMA target (10 cm long) ranged from z=-9 cm (beam entrance window) to z=+1 cm with BP position for ^{12}C at 120 MeV, 160 MeV, 180 MeV, and 220 MeV approximately at z=-6 cm, z=-4 cm, z=-3 cm, and z=0 cm, respectively.

file; x-y plane) is a convolution of the transverse profile of the primary beam (spot size), multiple scattering (MS) of the fragments in the PMMA target and DC tracking resolution, which has been studied in detail elsewhere [7]. The lateral profile can be used to evaluate the MS of the fragments inside the target knowing the remaining two contributions a priori.

3.2 Prompt-γ

Prompt-γ events were selected requiring less than three fired DC cells. The bi-dimensional distribution of energy deposited in the LYSO crystal for these events as a function of their TOF was used to select the prompt photons. An example of such a distribution for ^{12}C beam at 220 MeV/u is shown on Fig. 3 (left).

The prompt photon signal corrected by the slewing effect induced by the front-end electronics fixed voltage threshold is a vertical band at 0 ns. The LYSO intrinsic noise is visible as the horizontal low energy band, while the diffused cloud is mainly due to neutrons at ToF values greater than of prompt photons. The number of prompt photons has been extracted from an unbinned maximum likelihood fit to the time pull distribution for each energy bin and energy spectra of the prompt gamma emitted from all the beams were obtained.

In Fig. 3 (right) the energy spectrum for the prompt-γ emitted in the interaction of the ^{12}C beam with the PMMA target at 90° is shown. The observed spectra are given by the sum of the raw spectra corresponding to the nuclear de-excitation of both projectile and target fragments produced in the interaction of the ion beam with the PMMA target. While in Helium and Carbon beam interactions the target de-excitation is dominant, in the study of Oxygen spectral characteristics an non negligible contribution from projectile fragmentation was observed. Helium and Carbon energy spectra are in good agreement with the experimental results obtained with 80 MeV/u Carbon beam [9] and with 220 MeV/u Carbon beam [8].

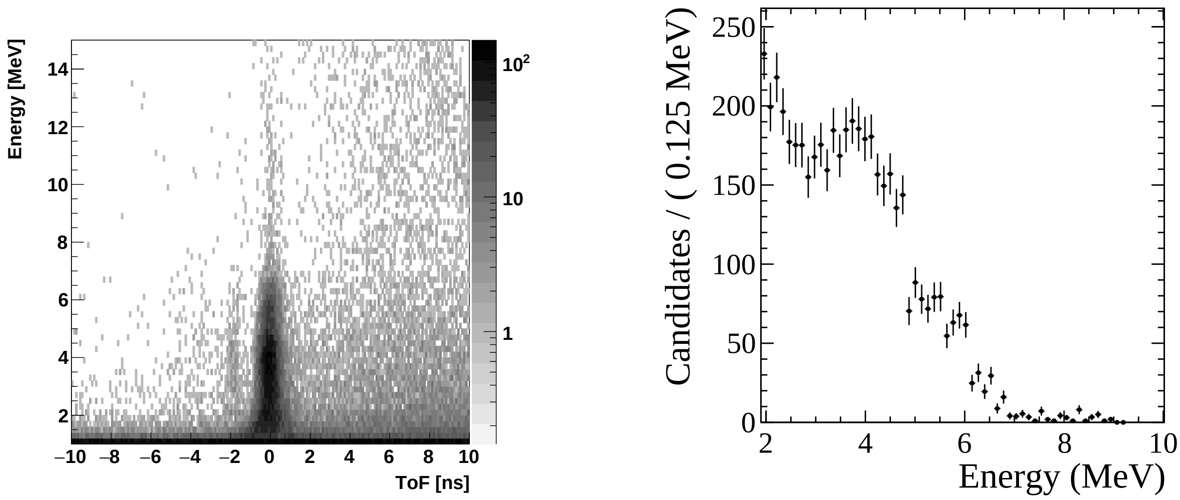

Fig. 3: LEFT Energy deposited in the LYSO crystal as a function of TOF. Vertical band at 0 ns corresponds to prompt-γ events. **RIGHT**: Energy spectrum of prompt-γ for ^{12}C beam at 220 MeV.

4. Dose Profiler - charged secondary on-line monitor

The non negligible production of charged secondary particles emitted by all the investigated primary beam interaction with a PMMA target allows to exploit the correlation of charged secondary protons emission profile with position of the primary beam for monitoring of the dose release in ion beam therapy.

For this purpose a tracking device, "Dose Profiler" (Fig. 1 right), made out of a scintillating fibers system, coupled to a calorimeter and realized by means of LYSO crystals matrix for measurement of particles energy was designed and is currently under construction. The materials of the detector were selected minimizing the charged particles multiple scattering in the detector. The Dose Profiler dedicated to track protons generated by the primary beam inside the patient consists of six planes of squared (0.5x0.5 mm^2) scintillating fibers (2 orthogonal layers in each plane) connected to silicon photo multipliers (SiPM) and read out by Basic32 front-end boards. The secondary proton detection and tracking efficiency is expected to be above 90%.

Depending on the position of the tumor in the patient, before reaching the detector the particles have to travel few centimeters inside the patient losing their energy. In order to reduce the impact of multiple scattering, the device design maximize the geometrical acceptance in order to improve statistics collected for a given dose to the patient.

5. Conclusions

During the test beam at HIT several millions of collisions of ^{12}C, ^{4}He and ^{16}O beams with a PMMA target were collected exploring the range of energies that is of interest for particle therapy. The experiment confirms an evidence of a non negligible secondary charged and prompt-γ production at 60° and 90° with respect to the primary beam, supporting the concept of on-line dose monitoring with those secondaries in ion beam therapy. The correlation of charged fragments emission profile with the position of Bragg Peak is possible with Helium, Carbon and Oxygen beams at all investigated energies. The development of a prototype monitoring system "Dose Profiler" dedicated for tracking of charged secondary particles on-line with a purpose of emission profile reconstruction is on the advanced stage. First tests, calibration and installation of the device in the treatment room of Centro Nazionale di Adroterapia

Oncologica (CNAO) is foreseen in 2016.

References

[1] M. Jermann, *Int J Particle Ther.*, available at the URL http://www.theijpt.org/doi/pdf/10.14338/IJPT-15-00013.
[2] J. S. Loeffler, M. Durante, *Nat Rev Clin Oncol*, http://dx.doi.org/10.1038/nrclinonc.2013.79.
[3] C. Kurz *et al.*, *Phys. Med. Biol.*, http://iopscience.iop.org/article/10.1088/0031-9155/57/15/5017.
[4] H. Fuchs *et al. Radiotherapy and Oncology*, http://dx.doi.org/10.1016/S0167-8140(15)30498-9.
[5] A.C. Knopf and A. Lomax *Phys. Med. Biol.*, http://iopscience.iop.org/article/10.1088/0031-9155/58/15/R131/pdf.
[6] K Parodi *et al.*, *IJROBP*, http://dx.doi.org/10.1016/j.ijrobp.2008.02.033.
[7] L. Piersanti *et al. Phys. Med. Biol.*, available at the URL http://iopscience.iop.org/article/10.1088/0031-9155/59/7/1857/pdf.
[8] I Mattei *et al. Accepted for publication in JINST*
[9] C Agodi *et al.* http://iopscience.iop.org/article/10.1088/1748-0221/7/03/P03001/pdf.
[10] C Agodi *et al.* http://iopscience.iop.org/article/10.1088/0031-9155/57/18/5667/pdf.
[11] Z Abou-Haidar *et al.*, http://iopscience.iop.org/article/10.1088/1748-0221/7/02/P02006/pdf.
[12] C. Agodi *et al.*, *Nucl. Instrum. Methods Phys. Res. B*, http://arxiv.org/pdf/1202.1676v2.pdf.